

Phases of a conserved mass model of aggregation with fragmentation at fixed sites

Kavita Jain and Mustansir Barma

*Department of Theoretical Physics, Tata Institute of Fundamental Research
Homi Bhabha Road, Mumbai 400005, India.*

To study the effect of quenched disorder in a class of reaction-diffusion systems, we introduce a conserved mass model of diffusion and aggregation in which fragmentation occurs only at certain fixed sites. On most sites, the mass moves as a whole to a nearest neighbour while it leaves the fixed sites only as a single monomer (i.e. chips off). Once the mass leaves any site, it coalesces with the mass present on its neighbour. The total mass of the system is conserved in this model as is evident from the rules. We study in detail the effect of a *single* chipping site on the steady state in arbitrary dimensions, with and without bias. In the thermodynamic limit, the system can exist in one of the following three phases – (a) Pinned Aggregate (PA) phase in which an infinite aggregate (i.e. an aggregate with mass proportional to the volume of the system) appears at the chipping site with probability one but not in the bulk. (b) Unpinned Aggregate (UA) phase in which *both* the chipping site and the bulk can support an infinite aggregate simultaneously. (c) Non Aggregate (NA) phase in which the system cannot sustain a cluster of mass proportional to the volume at all. The steady state of the system depends on the dimension and drive. A sitewise inhomogeneous Mean Field Theory predicts that the system exists in the UA phase in all cases. We tested this prediction by Monte Carlo simulations in $1d$ and $2d$ and found that it is true except in $1d$, biased case. In the latter case, there is a phase transition from the NA phase to the PA phase as the mass density is increased. We identify the critical point exactly and calculate the mass distribution in the PA phase. The NA phase and the critical point are studied by Monte-Carlo simulations and using scaling arguments. A variant of the above aggregation model is also considered in which total particle number is conserved and chipping occurs at a fixed site, but the particles do not interact with each other at other sites. This model is solved exactly by mapping it to a Zero Range Process. With increasing density, it exhibits a phase transition from the NA phase to the PA phase in all dimensions, irrespective of bias. The model is also solved with an extensive number of chipping sites with random chipping rates and we argue that the solution describes qualitatively the behaviour of the aggregation model with extensive disorder.

PACS numbers: 64.60.-i, 05.40.-a, 61.43.Hv

I. INTRODUCTION

Reaction-Diffusion systems form an important class of nonequilibrium systems whose dynamics and steady state depend on various factors such as the nature of the reaction (aggregation, annihilation, birth, fragmentation), number or type of reactants involved (single or multi-species), velocity of reactants (ballistic or diffusion controlled) and presence of external input (injection) [1–3]. An interesting class with wide ranging applications involves the elementary moves of *aggregation* (coalescence on contact) and *fragmentation* (break-up of clusters of masses), besides diffusion. A number of analytical results including the occurrence of nonequilibrium phase transitions have been obtained for such systems with translationally invariant geometries [4–8]. A natural question arises – what is the effect of quenched disorder on the possible phases of such systems and the transitions between them? We may anticipate interesting effects, as quenched disorder is known to strongly influence the character of the steady state in other nonequilibrium systems [9–14]. For instance, the steady state of driven diffusive systems on a one-dimensional lattice with bias shows phase separation in the presence of even a single defect [10,15–17].

To see what effect quenched disorder might have in a system with diffusion and aggregation, consider the process of polymerisation in a random medium with traps at certain fixed sites in which the polymer can get stuck. Aggregation occurs when two diffusing chains meet and coalesce; the reduced mobility of the aggregates at the trap sites promotes the formation of large, *localised* aggregates at such sites. If these traps are not perfect and allow monomers to detach and leave, there is also a possibility of formation of large *mobile* aggregates in the bulk.

To elucidate under what circumstances which types of aggregates may form as a result of these physical effects, namely, diffusion-aggregation, chipping and trapping, we consider a simple, reduced model in which the mass leaves as a single aggregate to a nearest neighbour from all sites except at certain, fixed sites from which it is allowed to leave only by single monomer dissociation. We refer to the loss of unit mass as chipping and these special sites as chippers. The total mass in the system is conserved as is evident from the dynamical rules described above. The quenched

character of the chipper sites is important in determining the steady state of this model which is quite different from that in the translationally invariant uniform-chipping model where chipping can occur at every site [7].

As a first step towards understanding such a spatially inhomogeneous system, we study in detail the case when only a *single* chipper is present. Despite the simplicity of the model, we find that the presence of a chipper gives rise to interesting steady states. We study the model both analytically and numerically in arbitrary dimensions, both with and without a global bias which sets up an overall mass current. The constraint of conservation of total mass in the model plays an important role in determining the steady state. We find that the system may exist in three possible phases. Depending on the dimension and the presence of drive, the system either stays in one of the phases or else make transitions from one phase to the another as the parameters are varied. These phases are characterised by the presence or absence of aggregates with mass proportional to the volume of the system. In the thermodynamic limit, the mass of such an aggregate diverges, so we refer to it as an infinite aggregate. The three phases are described below:

Pinned Aggregate phase (PA phase): In this phase, with probability one, an infinite aggregate occurs only at the chipper site and not in the bulk. This infinite aggregate acts as a spatially localised particle bath for rest of the system.

Unpinned Aggregate phase (UA phase): In this phase, a localised infinite aggregate can exist at the chipper site together with mobile infinite aggregates in the bulk. Interestingly, *both* types of infinite aggregate can exist simultaneously. In this sense, this state is different from the aggregate phases in translationally invariant systems such as the no-chipper limit of this model or the uniform chipping model [7], in which only one mobile infinite aggregate occurs at a time.

Non Aggregate phase (NA phase): This phase is characterised by the absence of an infinite aggregate anywhere in the system. The mass is spread out all over the system in clusters, each of which has a vanishing fraction of the total mass in the thermodynamic limit.

We analysed the system within a Mean Field Theory (MFT) allowing for the spatial dependence in the mass distributions. We find that the MFT predicts the existence of only the UA phase. On comparing this result with Monte Carlo simulations in $d = 1$ and $d = 2$, we find qualitative agreement except in the $1d$, biased case. In this exceptional case, there is a phase transition from the NA phase to the PA phase as the density is increased. This case is different from the rest due to an interesting interplay of the ballistic scale of motion and the diffusive scale of coalescence in one dimension.

In the model described above, an infinite aggregate is formed due to both interactions (coalescence of diffusing particles) and the presence of an inhomogeneity in the form of the chipper. It is useful to contrast the behaviour of this model with that of a model of *noninteracting* particles in which the aggregate is formed solely due to the presence of disorder. We solve this model in the presence of a single defect by mapping it to a Zero Range Process [14,18] and show that it exhibits a phase transition from the NA phase to the PA phase in all dimensions, irrespective of bias. This is in contrast to the aggregation model described earlier which does not show a phase transition in higher dimensions in the presence of single chipper.

Although we mainly discuss the case of a single chipper in this paper, we also discuss what happens in the presence of extensive disorder in both the models. We argue that in the presence of an extensive number of chippers, the interaction effects (i.e. coalescence) can be ignored in the aggregation model on large enough length and time scales and it behaves like the free-particle model. The latter model can be solved in the presence of extensive disorder and shows a phase transition in all dimensions for all bias from the PA phase to the NA phase as the density is decreased.

The remainder of the paper is organised as follows. We define the single-chipper aggregation model in Section II and discuss the possible phases on the basis of the conservation law. We analyse the system within a MFT in Section III and show that it predicts the occurrence of the UA phase. We also discuss the numerical results which support this broad conclusion in several cases. In Section IV we turn to the exceptional case namely the one dimensional, biased case. We present analytical results in the PA phase and numerical results in the NA phase and at the critical point. In Section V, we present the solution of the single-chipper free particle model. We also discuss the likely behaviour of the system with extensive disorder in Section VI. Finally we summarise our results in Section VII.

II. SINGLE-CHIPPER AGGREGATION MODEL AND ITS PHASES

A. The Model

Our model is defined on a d -dimensional hypercubic lattice of length L with periodic boundary conditions, and is studied both in the presence and absence of bias. The system evolves via following rules: at any site except the origin,

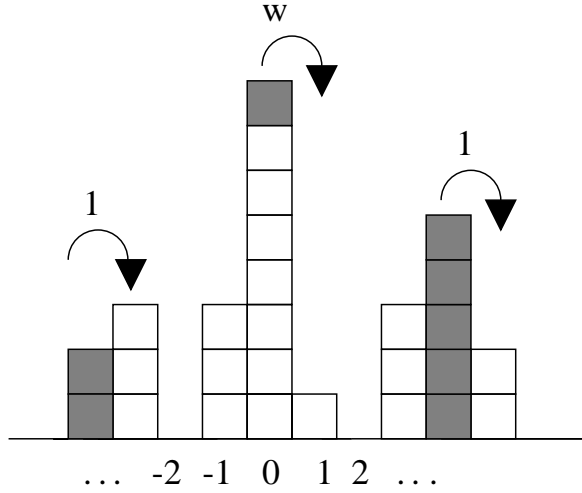


FIG. 1. Illustration of the aggregation and chipping moves in the totally biased case in one dimension. In an elementary move, only a monomer (shaded) can leave the chipper site (located at the origin) at a rate w . At sites other than the origin, the mass leaves as a whole (shaded) at a rate 1. Once the mass moves from any site to its neighbouring site, it coalesces with the mass already present on that site.

all the mass at that site moves as a whole to a nearest neighbour at a rate 1, while at the origin only a single monomer chips off at a rate w leaving rest of the mass behind. Once the mass moves from any site to its neighbouring site, it simply coalesces with the mass present on that site (see Fig. 1). Evidently, the total mass $M = \rho L^d$ of the system is conserved, where ρ is the mass density. The evolution of the system can be described by the time evolution equation for the probability $P_k(m, t)$ that there is mass m at site k at time t . As the moves at the origin are different from that at the rest of the system, the mass distribution at the origin (denoted by 0) and its nearest neighbours which receive mass from the origin (denoted by set A) obey equations different from those obeyed by rest of the system (set B).

The set of time evolution equations obeyed by the sites in the bulk (set B) are given by

$$\frac{\partial P_k(m, t)}{\partial t} = \sum_{\delta} \left[\sum_{m'=1}^m P_{k, k+\delta}(m - m', m', t) - \sum_{m' \neq 0} P_{k, k+\delta}(m, m', t) - P_k(m, t) \right], \quad k \in B \quad (1a)$$

$$\frac{\partial P_k(0, t)}{\partial t} = \sum_{\delta} \left[\sum_{m \neq 0} P_k(m, t) - \sum_{m' \neq 0} P_{k, k+\delta}(0, m', t) \right], \quad k \in B \quad , \quad (1b)$$

where $P_{k, k+\delta}(m, m', t)$ is the joint probability that site k and its nearest neighbour $k + \delta$ have mass m and m' respectively. The index δ runs over the $2d$ nearest neighbours in the unbiased case and d forward neighbours for totally biased case. The convolution term in Eq.(1a) is the gain term through which the deficit mass is supplied to site k via diffusion-aggregation moves from its nearest neighbours. The gain term for zero mass in Eq.(1b) results from hopping the mass from site k to one of its nearest neighbours. The system can get out of the configuration in which the site k has mass m (including zero) when (a) the mass hops into site k from its nearest neighbours and (b) the nonzero mass at site k hops to its nearest neighbours.

For the sites in the immediate neighbourhood of the origin (set A), the time evolution equation for $P_k(m, t)$ is similar to that for set B except that the contribution of the origin needs to be taken into account separately. We have

$$\begin{aligned} \frac{\partial P_k(m, t)}{\partial t} = & \sum_{\delta}' \sum_{m'=1}^m P_{k, k+\delta}(m - m', m', t) + w \sum_{m' \neq 0} P_{k, 0}(m - 1, m', t) - \sum_{\delta}' \sum_{m' \neq 0} P_{k, k+\delta}(m, m', t) \\ & - w \sum_{m' \neq 0} P_{k, 0}(m, m', t) - \sum_{\delta} P_k(m, t) \quad , \quad k \in A \end{aligned} \quad (2a)$$

$$\frac{\partial P_k(0, t)}{\partial t} = \sum_{\delta} \sum_{m \neq 0} P_k(m, t) - \sum_{\delta}' \sum_{m' \neq 0} P_{k, k+\delta}(0, m', t) - w \sum_{m' \neq 0} P_{k,0}(0, m', t) \quad , \quad k \in A \quad , \quad (2b)$$

where the primed sum denotes the sum over the nearest neighbours, excluding the origin. The contribution of the origin is taken care of by the terms with a coefficient w which accounts for the gain or loss in mass via chipping from the origin.

At the origin itself, the set of evolution equations obeyed are given by

$$\frac{\partial P_0(m, t)}{\partial t} = \sum_{\delta} \left[\sum_{m'=1}^m P_{0,0+\delta}(m-m', m', t) + w P_0(m+1, t) - \sum_{m' \neq 0} P_{0,0+\delta}(m, m', t) - w P_0(m, t) \right] \quad (3a)$$

$$\frac{\partial P_0(0, t)}{\partial t} = \sum_{\delta} \left[w P_0(1, t) - \sum_{m' \neq 0} P_{0,0+\delta}(0, m', t) \right] \quad . \quad (3b)$$

In the gain term for nonzero mass, besides the convolution term, there is an extra term due to the possibility of chipping off one extra monomer with a rate w . The loss terms are similar to those discussed for the sites in set B .

B. The Phases

One can obtain useful information about the nature of the steady state from the following simple analysis. In the steady state, the mass current into and out of any site must be equal, i.e.

$$\sum_{\delta} \langle m_k \rangle = \sum_{\delta} \langle m_{k+\delta} \rangle \quad , \quad k \in B \quad (4a)$$

$$\sum_{\delta} \langle m_k \rangle = w s_0 + \sum_{\delta}' \langle m_{k+\delta} \rangle \quad , \quad k \in A \quad (4b)$$

$$\sum_{\delta} w s_0 = \sum_{\delta} \langle m_{0+\delta} \rangle \quad , \quad (4c)$$

where $\langle m_k \rangle$ is the average mass at site $k \neq 0$ and $s_0 = 1 - P_0(0)$ is the probability that the origin is occupied. The solution of the above equations gives $\langle m_k \rangle = w s_0$ for all $k \neq 0$. Thus the average mass on a site in the bulk is uniform in spite of broken translational invariance. Since the total mass of the system is conserved, the average mass at the origin $\langle M_0 \rangle$ must satisfy

$$\langle M_0 \rangle = \rho L^d - w s_0 (L^d - 1) \quad . \quad (5)$$

Using this constraint equation, one can deduce some characteristics of the possible phases in the system as follows. Since the LHS in Eq.(5) is non-negative and s_0 is bounded above by one, the allowed domain for s_0 is constrained as shown in Fig. 2. Depending on the value of s_0 (and hence $\langle M_0 \rangle$), the system can exist in one of the three distinct phases described below.

PA phase: The system exists in this phase when s_0 is pinned to its maximum value 1 for all $\rho > w$ (shown by the bold line in Fig. 2). From the constraint equation Eq.(5), one deduces that the average mass at the origin grows as L^d giving rise to an infinite aggregate in the thermodynamic limit. Thus the Pinned Aggregate phase is defined as that in which an infinite aggregate is present at the origin with a probability one.

UA phase: The system exists in this phase for all values of s_0 lying in the shaded region in Fig. 2. This phase is characterised by s_0 strictly less than 1, and not equal to ρ/w . As in the PA phase, the average mass at the origin grows as L^d but s_0 is not fixed and varies with ρ . Since $s_0 < 1$, the infinite aggregate is present at the origin only for a finite fraction of the time. For this reason, we refer to this phase as the Unpinned Aggregate phase.

NA phase: This phase is characterised by $s_0 \rightarrow \rho/w$ as $L \rightarrow \infty$ (shown by the solid line in Fig. 2). Using Eq.(5), one immediately obtains $\langle M_0 \rangle / L^d \rightarrow 0$ in the thermodynamic limit. Due to the absence of an aggregate with mass of $O(L^d)$ at the origin, we call this the Non Aggregate phase.

A more detailed study of the system shows that depending on the dimension and drive, the system can either stay in one of the three phases or else make transitions from one phase to another as ρ is varied, keeping w fixed. We have solved for $\langle M_0 \rangle$ and s_0 in d dimensions within a sitewise inhomogeneous Mean Field Theory (Fig. 2) which predicts that the system exists only in the UA phase in all dimensions, regardless of the bias. This prediction was tested numerically in several cases and seen to be qualitatively correct except in the $1d$, biased case.

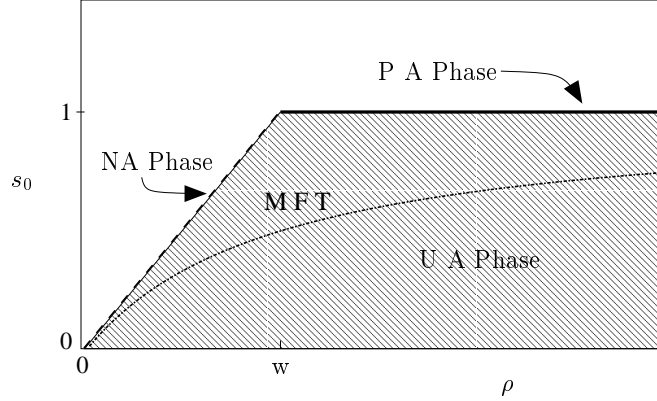


FIG. 2. Plot of s_0 vs. ρ to show the three possible phases in the steady state of the aggregation model in the thermodynamic limit. The system exists in (a) Pinned Aggregate phase when s_0 is one (bold horizontal line) (b) Unpinned Aggregate phase when $s_0 < 1$ and not equal to ρ/w (grey striped region) (c) Non Aggregate phase when s_0 is equal to ρ/w (dashed line). The smooth curve shows the MFT solution for $s_0 = \rho/(\rho + w)$ in the aggregation model.

In the latter case, there is a phase transition from the NA phase to the PA phase as one crosses the critical line $\rho = w$ either by increasing ρ with w held fixed or by decreasing w for fixed ρ .

III. UNPINNED AGGREGATE PHASE: MEAN FIELD THEORY AND MONTE-CARLO SIMULATIONS

In this Section, we analyse the aggregation model within the mean field approximation. We implement this approximation by replacing the joint probability distribution $P_{k,k+\delta}(m, m', t)$ by the product $P_k(m, t) P_{k+\delta}(m', t)$ of the single site probability distributions. We begin with the MFT analysis in arbitrary dimensions in Section III A. We will see that MFT predicts only the existence of the UA phase in all dimensions, irrespective of bias. In Section III B, we study the UA phase in one dimension in more detail. We discuss some limitations of this MFT and also present some numerical results. We close this Section with a qualitative discussion of the UA phase.

A. MFT in arbitrary dimensions

In this Section, we solve for $\langle M_0 \rangle$ and s_0 in arbitrary dimensions and for all bias within MFT and show that it predicts the occurrence of only the UA phase in all cases.

In the steady state, the mass distribution at any site k is independent of time and is determined by setting the LHS of Eqs.(1a)-(3b) equal to zero. Further we replace $P_{k,k+\delta}(m, m')$ by $P_k(m) P_{k+\delta}(m')$ in Eqs.(1a)-(3b) to obtain the mean field equations for $P_k(m)$. To study these equations, we define $Q_k(z) = \sum_{m=0}^{\infty} P_k(m) z^m$, the Laplace transform of $P_k(m)$ with respect to mass, and find that it obeys the following set of equations,

$$\sum_{\delta} Q_k = \sum_{\delta} [1 + Q_k (Q_{k+\delta} - 1)] \quad , \quad k \in B \quad (6a)$$

$$Q_k = \frac{\sum_{\delta} 1}{\sum_{\delta} 1 + w s_0 (1 - z) - \sum_{\delta} (Q_{k+\delta} - 1)} \quad , \quad k \in A \quad (6b)$$

$$Q_0 = \frac{\sum_{\delta} w (1 - z) (1 - s_0)}{\sum_{\delta} [w (1 - z) + z (Q_{0+\delta} - 1)]} \quad . \quad (6c)$$

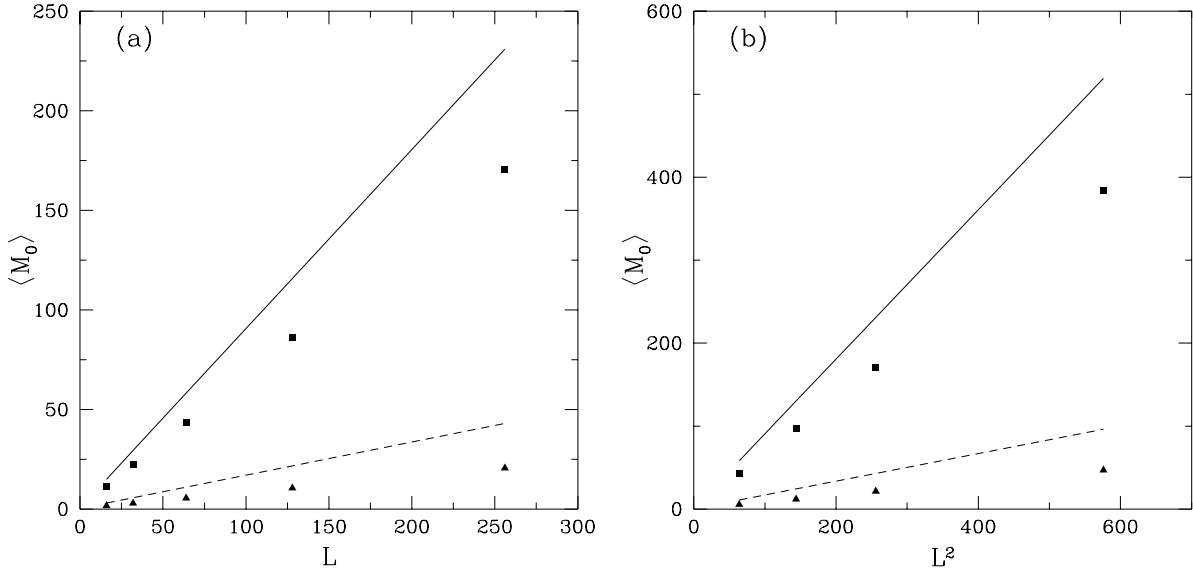


FIG. 3. Plot of $\langle M_0 \rangle$ vs. L^d for the symmetric, aggregation model for (a) $d = 1$ and (b) $d = 2$. In each case, the numerical result is plotted for two densities $\rho = 1.5$ (squares) and $\rho = 0.5$ (triangles) along with the MFT prediction (solid line for $\rho = 1.5$ and broken line for $\rho = 0.5$). Set of parameters used: $w=1$.

Since $P_k(m)$ is normalised to one, $Q_k(1) = 1$ for all k in the above equations. The average mass in the bulk $\langle m_k \rangle = Q'_k(z)|_{z=1}$ still obeys Eqs.(4a)-(4c) which gives uniform mass in the bulk $\langle m \rangle = ws_0$, and Eq.(5) still holds.

Although we could not solve the above set of nonlinear coupled equations, we were able to compute two quantities of primary interest, namely, $\langle M_0 \rangle$ and s_0 . We begin by observing that the average mass at the origin can be written in terms of the mean-squared mass at its nearest neighbours,

$$\langle M_0 \rangle = \frac{\sum_{\delta} (2ws_0 + \langle m_{0+\delta}^2 \rangle - \langle m \rangle)}{\sum_{\delta} 2w(1 - s_0)} \quad , \quad (7)$$

where we have used that $\langle M_0 \rangle = Q'_0(z)|_{z=1}$ and $\langle m_k^2 \rangle = Q''_k(z)|_{z=1} + \langle m \rangle$, $k \neq 0$.

The mean-squared mass at sites other than the origin obeys the following set of *linear* equations,

$$\sum_{\delta} \langle m_k^2 \rangle = \sum_{\delta} \left(\langle m_{k+\delta}^2 \rangle + 2\langle m \rangle^2 \right) \quad , \quad k \in B \quad (8a)$$

$$\sum_{\delta} \langle m_k^2 \rangle = \sum_{\delta}' \left(\langle m_{k+\delta}^2 \rangle + 2\langle m \rangle^2 \right) + 2\langle m \rangle^2 + \langle m \rangle \quad , \quad k \in A \quad . \quad (8b)$$

It suffices to calculate $\sum_{\delta} \langle m_{0+\delta}^2 \rangle$ in order to obtain $\langle M_0 \rangle$. Adding the above $L^d - 1$ equations, one obtains

$$\sum_{\delta} \langle m_{0+\delta}^2 \rangle = \sum_{\delta} \left(2\langle m \rangle^2 (L^d - 1) + \langle m \rangle \right) \quad , \quad (9)$$

which further yields

$$\langle M_0 \rangle = \frac{ws_0 + \langle m \rangle^2 (L^d - 1)}{w(1 - s_0)} = \rho L^d - ws_0 (L^d - 1) \quad , \quad (10)$$

where the mass conservation equation Eq.(5) has been used in the last identity. Solving for s_0 and $\langle M_0 \rangle$ in terms of ρ, w and L , we find

$$\langle M_0 \rangle = \frac{\rho L^d (1 + \rho L^d)}{(1 - w) + (\rho + w)L^d} \quad (11a)$$

$$s_0 = \frac{\rho L^d}{(1 - w) + (\rho + w)L^d} \quad . \quad (11b)$$

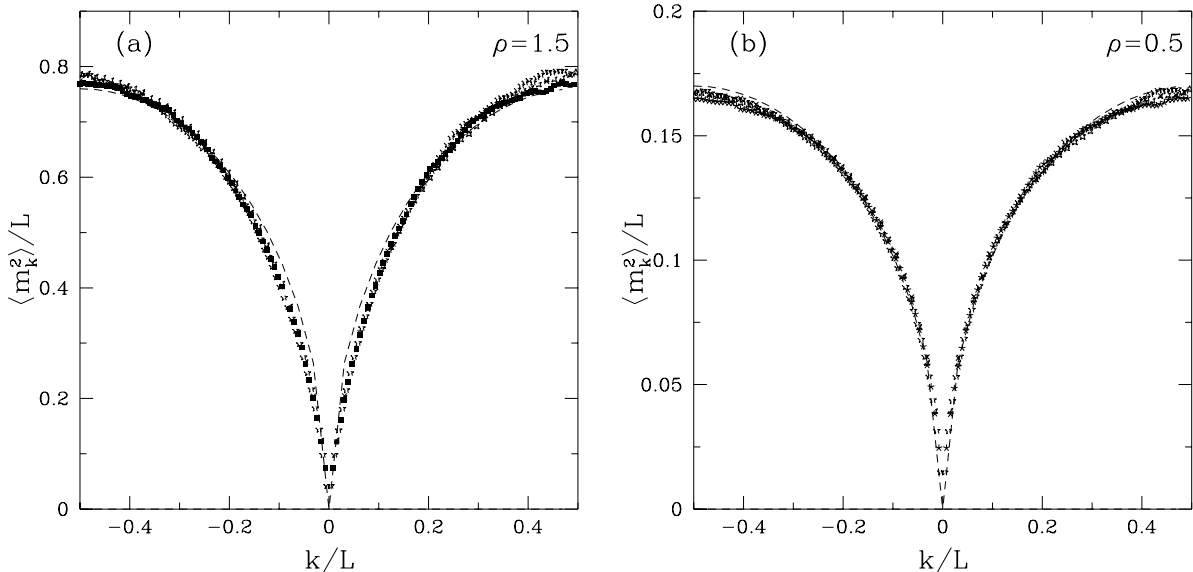


FIG. 4. Data collapse for the mean squared mass at site $k \neq 0$ for $1d$, symmetric aggregation model for $L = 32, 64, 128, 256$ for (a) $\rho = 1.5$ and (b) $\rho = 0.5$. The numerical fit $y = A(\rho) \sqrt{x(1-x)}$ where $x = |k|/L$ is shown in broken line with $A(\rho = 1.5) = 1.52$ and $A(\rho = 0.5) = 0.34$. Set of parameters used: $w=1$.

To lowest nonvanishing order in L , the above equations give $\langle M_0 \rangle \sim L^d$ and $s_0 < 1$ which are the signatures of the UA phase. Thus MFT predicts that the system exists only in the UA phase for all ρ and w (see Fig. 2). Our numerical simulations show that this prediction is true at least qualitatively in all cases except in the $1d$, biased case. In Fig. 3, we show our simulation results for $\langle M_0 \rangle$ in the absence of bias in $1d$ and $2d$ plotted along with the MFT results, and find qualitative agreement. We also measured s_0 for various system sizes and densities, fixing $w = 1$ and find that it is independent of L in accordance with Eq.(11b). For $\rho = 0.5$, we found that $s_0^{num} \simeq 0.42$ to be compared with $s_0^{MFT} \simeq 0.33$; for $\rho = 1.5$, numerically $s_0^{num} \simeq 0.84$ whereas $s_0^{MFT} = 0.6$.

B. UA phase in one dimension

In this Section, we analyse the UA phase in more detail in the $1d$, unbiased case. We solve Eq.(8a) and Eq.(8b) for the mean-squared mass in the bulk in this case and find that the MFT seems to violate the conservation law. We comment on this limitation of MFT. We also present numerical evidence which shows the simultaneous presence of more than one infinite aggregate in the system.

For convenience, we will choose L to be odd. The mean-squared mass at sites other than the origin obeys the following equations,

$$2\langle m_k^2 \rangle = \langle m_{k-1}^2 \rangle + \langle m_{k+1}^2 \rangle + 4\langle m \rangle^2, \quad |k| \geq 2 \quad (12a)$$

$$2\langle m_1^2 \rangle = \langle m_2^2 \rangle + \langle m \rangle + 4\langle m \rangle^2 \quad (12b)$$

$$2\langle m_{-1}^2 \rangle = \langle m_{-2}^2 \rangle + \langle m \rangle + 4\langle m \rangle^2 \quad (12c)$$

This set of equations can be solved and one obtains

$$\langle m_k^2 \rangle = 2\langle m \rangle^2(L-1) + 2\langle m \rangle^2(|k|-1)(L-|k|-1) + \langle m \rangle, \quad k \neq 0 \quad (13)$$

To leading order in L , the above result can be written in the scaling form $\langle m_k^2 \rangle = L^2 f(|k|/L)$ where $f(x) = x(1-x)$ [19].

The mean squared mass $\langle m_k^2 \rangle$ is actually a measure of the typical mass at site k . To see this, note that we may define two types of average over mass distributions at site k , namely, an average $\langle \dots \rangle$ over all mass occupations including $m_k = 0$, and an average $\langle \langle \dots \rangle \rangle$ over mass occupations excluding $m_k = 0$. It is straightforward to see that $\langle \langle \dots \rangle \rangle = \langle \dots \rangle / s_k$ where $s_k = 1 - P_k(0)$ is the probability that site k is occupied. For instance, the average mass $\langle m_k \rangle$

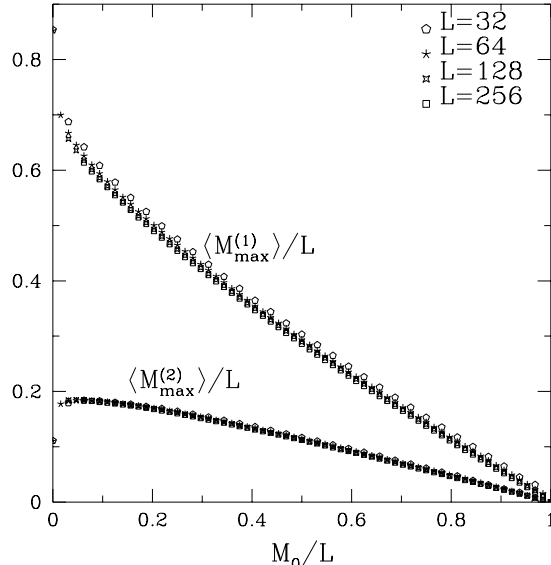


FIG. 5. Data collapse for the conditional average masses $\langle M_{max}^{(1)} \rangle$ and $\langle M_{max}^{(2)} \rangle$ of the clusters of largest and second largest mass in the bulk when the mass at the chipper is M_0 for $1d$, symmetric aggregation model for $L = 32, 64, 128, 256$. Set of parameters used: $w=1, \rho = 1$.

is same on all sites while the typical mass $\langle\langle m_k \rangle\rangle = \langle m_k \rangle / s_k$ will depend on k . Similarly, $\langle\langle m_k^2 \rangle\rangle$ is the square of the typical mass at site k , implying that $\langle m_k^2 \rangle = \langle\langle m_k^2 \rangle\rangle s_k$ may be interpreted as a measure of the typical mass at site k .

We performed numerical simulations to test the mean field prediction for the scaling form $\langle m_k^2 \rangle = L^2 f(|k|/L)$ where $f(x) = x(1-x)$. As shown in Fig. 4, we obtain a data collapse with the scaling form $\langle m_k^2 \rangle = Lg(|k|/L)$ with $g(x) \sim \sqrt{x(1-x)}$ as the numerical fit for the scaling function. Since $g(x) \sim \sqrt{x}$ for x close to zero and is constant for $x \approx 1/2$, the typical mass scales as \sqrt{L} for k close to the origin but as L at sites diametrically opposite to the origin. This points to the existence of an aggregate in the bulk as well, consistent with the nomenclature Unpinned Aggregate Phase.

One notes that the MFT solution seems to violate the conservation law since it predicts typical masses of $O(L^2)$ at sites situated $O(L)$ away from the chipper. On the other hand, one can also check that Eq.(5) is true using the MFT results for $\langle M_0 \rangle$ and s_0 . Thus MFT seems to be able to describe the vicinity of the chipper more correctly than the bulk. The reason for this could be that the mass fluctuations about the mean near the chipper are small due to fragmentation unlike those in the bulk where only the aggregation move operates. At a distance of $O(L)$ away from the chipper, to a good approximation, one can neglect the presence of the chipper. Then as all the mass resides only on one site, the mass-mass correlation function at two different sites $\langle m_i m_j \rangle$ is exactly zero in the steady state, in strong contrast to the mean field approximation $\langle m_i m_j \rangle = \langle m \rangle^2$. Thus a more refined approximation is required in the regions where the aggregation move dominates.

In Fig. 5, we present the numerical evidence which indicates the simultaneous presence of more than one infinite aggregate in the system. We measured the conditional average masses $\langle M_{max}^{(1)} \rangle$ and $\langle M_{max}^{(2)} \rangle$ of the clusters of the largest and second largest mass in the bulk respectively, given there is a mass M_0 at the chipper. We find that data collapse is obtained with the scaling forms $\langle M_{max}^{(1)} \rangle = Lf_1(M_0/L)$ and $\langle M_{max}^{(2)} \rangle = Lf_2(M_0/L)$, where the scaling functions $f_1(x)$ and $f_2(x)$ decay almost linearly. Thus a localised infinite aggregate at the chipper and one or more mobile infinite aggregates in the bulk can be present at the same time; we would expect more than one infinite aggregate to be present in higher dimensions as well.

In any dimension d , far away from the chipper site, the state resembles that in the absence of the chipper. In the latter case, there is a single mobile infinite aggregate which is equally likely to be present at any site with a probability $1/L^d$. Although this mobile aggregate with mass of order L^d arrives at the chipper infrequently, the probability of occupation s_0 of the chipper is of $O(1)$ – this enhancement occurs because mass can leave only one unit at a time, so that it stays for a time of at least order L^d . It is implicit in the above argument that an infinite aggregate can be formed in the bulk before it hits the chipper. However, this fails to be true in the $1d$, biased case which explains the absence of the UA phase in that case.

IV. ASYMMETRIC SINGLE-CHIPPER AGGREGATION MODEL IN ONE DIMENSION

The mean field prediction that the system exists in the UA phase fails in $1d$, biased case. In the presence of a drift velocity, the one-dimensional system undergoes a phase transition from the NA phase to the PA phase as ρ is increased, keeping w fixed. This exceptional case is the subject of this Section. Although the phase transition survives for all nonzero bias, we will only discuss the extreme case when the mass moves only forward (i.e. infinite bias).

The time required to form an aggregate with mass of $O(L)$ in the bulk is $O(L^2)$. But in this case, due to ballistic motion, the mass clusters return to the chipper in time of $O(L)$ ruling out the formation of an infinite aggregate in the bulk. For small w , the sublinear mass arriving at the chipper cannot leave it easily and is temporarily trapped giving rise to a localised infinite aggregate (PA phase). As w is increased, the mass leaves more frequently rendering the trapping less effective; also this chipped off mass cannot return before the chipper gets empty so that an infinite aggregate cannot be sustained at the chipper for large w (NA phase). Thus there is a phase transition in the $1d$, biased case as w (or alternatively ρ) is varied.

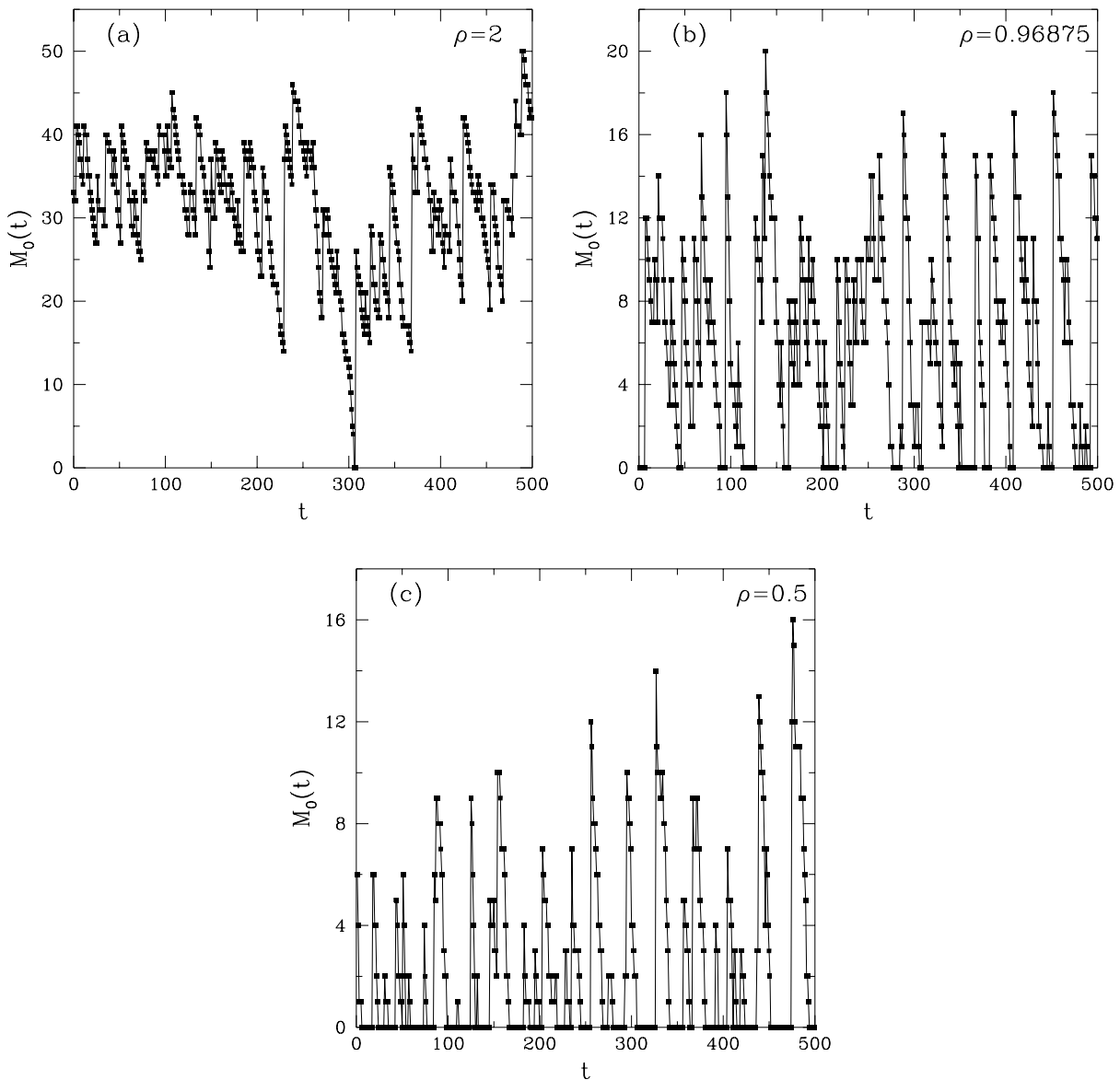


FIG. 6. Instantaneous mass at the origin $M_0(t)$ vs. t in the steady state of $1d$, asymmetric aggregation model. (a) The PA phase ($\rho = 2$). (b) The critical point ($\rho = 0.96875$). (c) The NA phase ($\rho = 0.5$). Set of parameters used: $L=32$, $w=1$.

The critical point is determined exactly to be at $\rho_c = w$ in the thermodynamic limit by setting the LHS to be zero and $s_0 = 1$ in Eq.(5). For $\rho < \rho_c$, the system exists in the NA phase which is characterised by $s_0 = \rho/w$ and $\langle M_0 \rangle$ growing sublinearly with L . For $\rho > \rho_c$, the system exists in the PA phase in which s_0 is pinned to its maximum value 1 and $\langle M_0 \rangle$ grows linearly with L (see Fig. 2). The probability $P_0(0) = 1 - s_0$ that the origin is empty serves as an order parameter. Our numerical simulations indicate that to lowest order in L ,

$$1 - s_0 = P_0(0) \sim \begin{cases} O(e^{-L/L_0}) & , \rho > w \\ O(L^{\beta-1}) & , \rho = w \\ \text{constant} & , \rho < w \end{cases} . \quad (14)$$

Since $P_0(0)$ varies continuously from the NA phase to PA phase as ρ increases, this is a second order phase transition.

Before delving into details, we first present a pictorial representation of the phases. Let us imagine monitoring the instantaneous mass at the chipper site in the steady state. Figure 6 shows the time series for the mass at the origin as a function of time in the two phases and at the critical point. The mass at the chipper increases due to the mass input from the site behind the chipper, and decreases due to fragmentation. Let t_0 and t_1 respectively denote the consecutive number of time steps during which the chipper is empty and occupied. Then s_0 can be related to t_0 and t_1 through $s_0^{-1} - 1 = \langle t_0 \rangle / \langle t_1 \rangle$. Depending on whether the ratio $\langle t_0 \rangle / \langle t_1 \rangle$ is zero or not in the thermodynamic limit, s_0 is either pinned to 1 (PA phase) or strictly less than 1 (NA phase). In the PA phase, $\langle t_1 \rangle / \langle t_0 \rangle \gg 1$ holds due to long cascades of successive mass inputs, thus enabling the origin to maintain s_0 equal to 1. The long t_1 stretches (see Fig. 6(a)) enables the chipper to build an aggregate with mass of order of system size. In contrast, in the NA phase, $\langle t_0 \rangle \gtrsim \langle t_1 \rangle$ holds as depicted in Fig. 6(b) by the stretches of time during which the origin is empty (due to absence of multiple inputs) which reduces s_0 from its maximum value 1. Since t_1 is typically not very long, the chipper cannot sustain an infinite aggregate in NA phase. Finally, at the critical point, there are multiple mass inputs to the chipper but these cascades are not very long as shown in Fig. 6(c). We now turn to a systematic discussion of each phase.

A. The Pinned Aggregate Phase

Since the total mass in the system is conserved and the $L - 1$ sites in the bulk have nonzero average mass $\langle m \rangle$ and sublinear fluctuations about the mean mass (due to absence of a cluster of mass of order L in the bulk as argued above), the probability $P_0(m)$ that the origin has mass m is $\sim 1/\sqrt{L} \exp(-(m - m_0)^2/L)$ where $m_0 \sim M - \langle m \rangle L$ which gives $P_0(0) \sim \exp(-L)$. Thus in this phase, the chipper site is occupied with probability one in the thermodynamic limit so that it acts as a reservoir of particles for the bulk. One can think of the system as a semi-infinite, one dimensional lattice with a perfect, localised source at the origin injecting monomers into it at the rate w .

The problem of aggregation in the presence of such a source has been considered previously as well. Some properties were studied in [20] using the technique of interparticle distribution function (IPDF) introduced in [22], and in [21] by mapping this $1d$ problem to a bounded random walk in $2d$. Here we calculate the steady state mass distribution at site k denoted by $P_k(m)$ by the generating function method. We define the r -point characteristic function for site k at time t , $Z_r^{(k)}(\lambda, t) = \langle e^{-\lambda \sum_{j=k}^{k+r-1} m_j(t)} \rangle$. The time evolution equations obeyed by $Z_r^{(k)}(\lambda, t)$ with a perfect, localised source at $k = 0$ are given by

$$\frac{\partial Z_r^{(k)}}{\partial t} = Z_{r+1}^{(k-1)} + Z_{r-1}^{(k)} - 2Z_r^{(k)} \quad , \quad k \neq 1 \quad , \quad r \neq 0 \quad (15a)$$

$$\frac{\partial Z_r^{(1)}}{\partial t} = Z_{r-1}^{(1)} + (we^{-\lambda} - 1 - w)Z_r^{(1)} \quad , \quad r \neq 0 \quad (15b)$$

with the boundary condition $Z_0^{(k)}(\lambda, t) = 1$ for all $k > 0$. In the steady state, $Z_r^{(k)}(\lambda, t)$ is independent of t .

We need to solve for $Z_1^{(k)}(\lambda)$ which is the Laplace transform of $P_k(m)$ with respect to m . One can easily solve for $Z_1^{(1)}(\lambda)$ using Eq.(15b) and the boundary condition $Z_0^{(1)} = 1$ which on taking the inverse Laplace transform for large m gives $P_1(m) = e^{-m/w}/w$. Thus the mass distribution at the first site decays exponentially. Now to find the probability distribution in the bulk, we define

$$H(x, y, \lambda) = \sum_{k=2, \dots} \sum_{r=1, \dots} Z_r^{(k)}(\lambda) x^k y^r \quad . \quad (16)$$

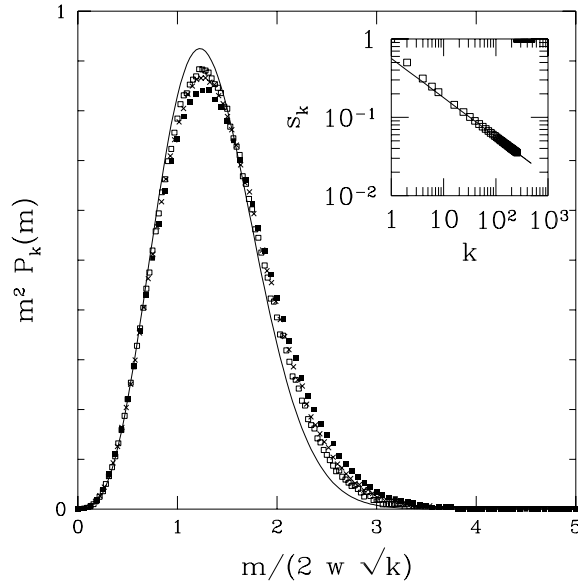


FIG. 7. Data collapse for the unnormalised probability distribution of mass at site $k = 64$ (solid squares), 128 (crosses), 256 (squares) in the PA phase plotted against the analytical result. Inset: log-log plot of probability distribution for nonzero mass at site k plotted against the analytical result. Set of parameters used: $L = 256$, $\rho = 2$, $w = 1$.

Using equations Eq.(15a) and Eq.(15b), one obtains

$$H(x, y, \lambda) = \frac{xy}{y^2 - 2y + x} \left[G(x, \lambda) - xy \left(\frac{1}{1-x} + \frac{f^2}{1-fy} \right) \right], \quad (17)$$

where $1/f = 1 + w - we^{-\lambda}$ and $G(x, \lambda) = \sum_{k=2, \dots} Z_1^{(k)}(\lambda) x^k$. Clearly, the inverse Laplace transform of $G(x, \lambda)$ w.r.t. λ and x gives $P_k(m)$ for $k > 1$. To calculate $G(x, \lambda)$, we use the same method as in [23]. We first note that the denominator of $H(x, y, \lambda)$ has roots at $y_{\pm} = 1 \pm \sqrt{1-x}$. The root at $y = y_-$ lies inside the unit circle which in the real space (i.e. r -space) gives an exponentially increasing solution which is disallowed since the inverse Laplace transform of $H(x, y, \lambda)$ gives a probability, which is always bounded above. To avoid this pathological solution, we demand that $y = y_-$ is a zero of the numerator as well, i.e.

$$G(x, \lambda) = xy_- \left(\frac{1}{1-x} + \frac{f^2}{1-fy_-} \right). \quad (18)$$

For $\lambda \rightarrow 0$ and $x \rightarrow 1$, the inverse Laplace transform can be easily found. We find that $P_k(m)$ has a scaling form $\phi(u)/m^2$ where $u = m/2w\sqrt{k}$ and the scaling function is

$$\phi(u) = \frac{4w}{\sqrt{\pi}} u^3 e^{-u^2}. \quad (19)$$

One can also obtain the probability distribution $P_k(0)$ of zero mass at site k by solving for $G(x, \lambda)$ when $\lambda \rightarrow \infty$ and $x \rightarrow 1$. To leading order in k , one obtains $P_k(0) = 1 - s_k = 1 - 1/\sqrt{\pi k}$. We tested our calculations against the numerical simulations performed on the single-chipper model and found reasonably good agreement (see Fig. 7). Thus the typical mass at site k grows as \sqrt{k} .

We now calculate the typical spacing between the masses using the method of IPDF [22]. We define $E_k(r, t)$ as the probability that the sites k to $k+r$ are empty (including k and $k+r$). Then $E_k(r, t)$ satisfies the following equations,

$$\frac{\partial E_k(r, t)}{\partial t} = E_k(r-1, t) - 2E_k(r, t) + E_{k-1}(r+1, t), \quad k \neq 1 \quad (20a)$$

$$\frac{\partial E_1(r, t)}{\partial t} = E_1(r-1, t) - (1+w)E_1(r, t), \quad (20b)$$

with the boundary condition $E_k(-1, t) = 1$ for all $k > 0$. In the steady state, $E_k(r, t)$ is independent of t and one can write the above equation in terms of $F_1(z, y) = \sum_{k=2, \dots} \sum_{r=0, \dots} E_k(r) z^k y^r$ and $R(z, r) = \sum_{k=2, \dots} E_k(r) z^k$, $r = 0, 1, \dots$. We find

$$F_1(z, y) = \frac{y}{y^2 - 2y + z} \left[\frac{zR(z, 0)}{y} - \frac{z^2}{(1+w)(1+w-y)} - \frac{z^2}{1-z} \right] . \quad (21)$$

With the same reasoning as in the previous calculation, we demand that the numerator of $F_1(z, y)$ evaluated at $y_- = 1 - \sqrt{1-z}$ be zero. This condition gives

$$R(z, 0) = \left[\frac{1}{1-z} + \frac{1}{(1+w)(1+w-y_-)} \right] z y_- , \quad (22)$$

which on inverting the Laplace transform gives the probability $E_k(0)$ which is same as $P_k(0)$. One can check that the result for $P_k(0)$ quoted above is reproduced. Substituting $R(z, 0)$ in $F_1(z, y)$, we obtain

$$F_1(z, y) = \frac{-z^2}{y - y_+} \left[\frac{1}{1-z} + \frac{1}{(1+w-y)(1+w-y_-)} \right] , \quad (23)$$

where $y_+ = 1 + \sqrt{1+z}$.

We further define $D_k(r)$ as the probability that both sites k and $k+r$ are occupied but no sites in between. Then

$$D_k(r) = E_{k+1}(r-2) - E_{k+1}(r-1) - E_k(r-1) + E_k(r) , \quad k \neq 1, r \neq 0 . \quad (24)$$

Defining the Laplace transform of $D_k(r)$ with respect to k and r as $F_2(z, y) = \sum_{k=2, \dots} \sum_{r=0, \dots} D_k(r) z^k y^r$, we obtain

$$F_2(z, y) = \frac{1}{z} \left(R(z, -2) + \frac{yz^2}{1-z} \right) - \frac{z(1+z)}{1-z} + F_1(z, y) \left(\frac{y^2}{z} + (1-y)(1 + \frac{1}{z}) \right) \\ + z(1-y) \left(1 + \frac{y}{2-y} \left\{ 1 + \frac{1}{(1+w)(1+w-y)} \right\} \right) , \quad (25)$$

where $F_1(z, y)$ was calculated above.

Then the typical empty space $\langle r_k \rangle$ in front of site k can be obtained by taking the inverse Laplace transform of $(\partial F_2 / \partial y)|_{y=1}$ with respect to z . One finds

$$\langle r_k \rangle = 1 + \frac{2}{\sqrt{\pi k}} - w e^{w^2 k} \operatorname{erfc}(w\sqrt{k}) , \quad (26)$$

which for large k implies that the typical empty space $\langle\langle r_k \rangle\rangle = \langle r_k \rangle / s_k$ in front of occupied site k varies as \sqrt{k} .

Thus, in the PA phase, the mass in the bulk is distributed in \sqrt{L} clusters with typical mass \sqrt{k} at site k , and an empty stretch of length \sqrt{k} in front of it.

B. The Non Aggregate Phase

As discussed earlier, in the NA phase, s_0 is strictly less than 1 due to substantial time stretches of typical length $\langle t_0 \rangle$ during which the origin is not occupied (Fig. 6). Thus the origin does not act as a perfect source unlike in the PA phase and we could not calculate the mass distribution in this phase. However, one can obtain useful information about the nature of this phase by simple scaling arguments. We begin by arguing that $\langle M_0 \rangle$ grows sublinearly with L and then provide numerical evidence for the absence of an infinite aggregate (i.e. mass proportional to L) in the bulk, thus concluding that there is no infinite aggregate anywhere.

Monte Carlo simulations indicate that $\langle M_0 \rangle$, $\langle t_0 \rangle$ and $\langle t_1 \rangle$ vary as a power law in L with a constant as a next order correction (see Fig. 9). Therefore, we assume $\langle M_0 \rangle = aL^\beta + b$, $\langle t_0 \rangle = c_0 L^\gamma + d_0$ and $\langle t_1 \rangle = c_1 L^\eta + d_1$. Solving for s_0 using Eq.(5), we obtain

$$s_0 = \frac{\rho}{w} + O\left(\frac{1}{L^{1-\beta}}\right) . \quad (27)$$

Then since the lowest order term for s_0 is a constant and $s_0^{-1} - 1 = \langle t_0 \rangle / \langle t_1 \rangle$, one obtains $\gamma = \eta$. Using this identity and retaining terms to lowest order in L we further obtain

$$s_0 = \frac{c_1}{c_0 + c_1} + O\left(\frac{1}{L^\gamma}\right) . \quad (28)$$

Comparison of Eq.(27) and Eq.(28) yields $\beta + \gamma = 1$.

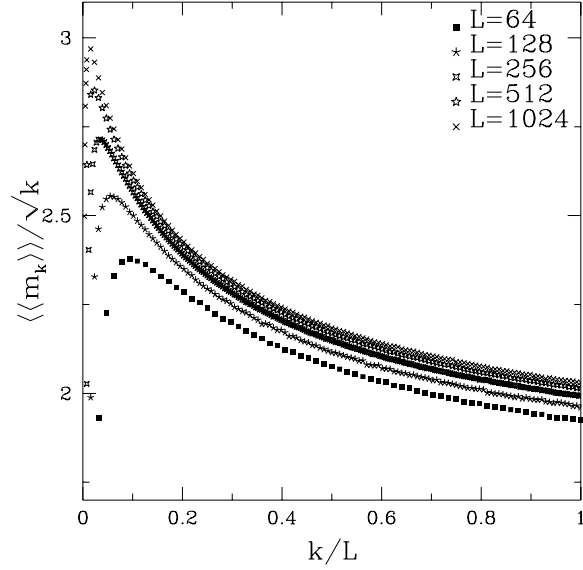


FIG. 8. Data collapse for the typical mass at site $k \neq 0$ in the NA phase for $L = 64, 128, 256, 512, 1024$. Set of parameters used: $\rho = 1, w = 2$. In this figure, all the sites are labelled by positive integers in the clockwise direction with the chipper at the origin.

Now we consider the typical mass $\langle\langle m_k \rangle\rangle$ in the bulk where the site index k is labelled by positive integers in the clockwise direction with the chipper at the origin. Numerically, $\langle\langle m_k \rangle\rangle$ is observed to obey the scaling form, $\langle\langle m_k \rangle\rangle = \sqrt{k} f(k/L)$ as shown in the data collapse in Fig. 8. The scaling function is a slowly varying function, which gives sublinear mass everywhere in the bulk. Thus in the NA phase, the mass is distributed in clusters of typical mass $\sim O(\sqrt{L})$ for $k \sim O(L)$.

Since the mass at the site just behind the chipper is of $O(\sqrt{L})$ and as one can see in Fig. 6, the number of mass inputs to the chipper is typically of $O(1)$, it follows that $\langle t_1 \rangle \sim O(\sqrt{L})$ so that $\eta = 0.5$, which further gives $\beta = \gamma = \eta = 0.5$ due to the two scaling relations above. These exponent values are checked numerically, as shown in Fig. 9.

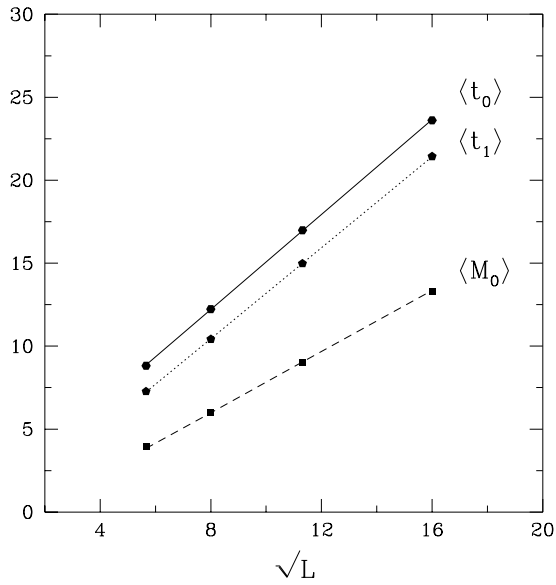


FIG. 9. Plot of $\langle M_0 \rangle, \langle t_0 \rangle$ and $\langle t_1 \rangle$ as a function of \sqrt{L} in the NA phase. Since all the three curves are linear, it follows that $\langle M_0 \rangle = aL^\beta + b$, $\langle t_0 \rangle = c_0 L^\gamma + d_0$ and $\langle t_1 \rangle = c_1 L^\eta + d_1$ with $\beta = \gamma = \eta = 0.5$. Set of parameters used: $\rho = 1, w = 2$.

C. The Critical Point

We studied the critical point mainly numerically by studying the L dependence of $\langle M_0 \rangle$, $\langle t_0 \rangle$ and $\langle t_1 \rangle$. Assuming a power law dependence for $\langle M_0 \rangle \sim L^\beta$, $\langle t_0 \rangle \sim L^\gamma$ and $\langle t_1 \rangle \sim L^\eta$, a naive best fit in the range $L = 32$ to 2048 gives $\beta \simeq 0.62$, $\gamma \simeq 0.38$ and $\eta \simeq 0.80$. However, the effective exponent calculated using the successive ratios of L used in the simulations shows systematic trends: β decreases as L increases while both γ and η increase with L .

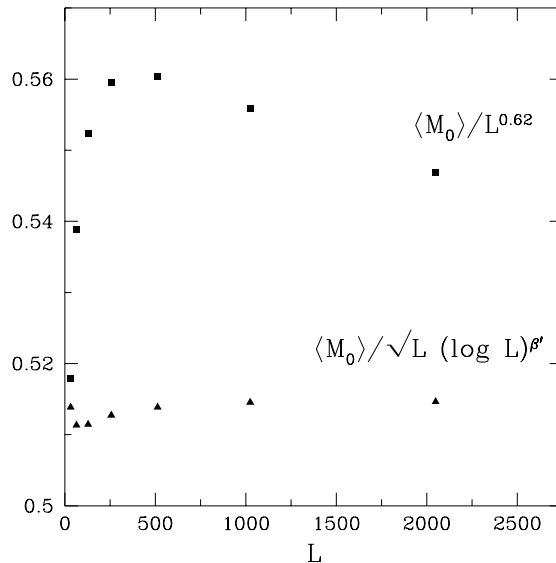


FIG. 10. Plot of $\langle M_0 \rangle / L^{0.62}$ (squares) and $\langle M_0 \rangle / \sqrt{L} (\log L)^{\beta'}$, $\beta' \simeq 0.7$ (triangles) as a function of L at the critical point in the 1d, biased case. The variation of $\langle M_0 \rangle$ as \sqrt{L} with multiplicative logarithmic correction seems to be a better fit than the fit to a pure power law. The plot of $\langle M_0 \rangle / L^{0.62}$ vs. L has been scaled by a constant factor. Set of parameters used: $\rho = 1, w = \rho L / (L - 1)$.

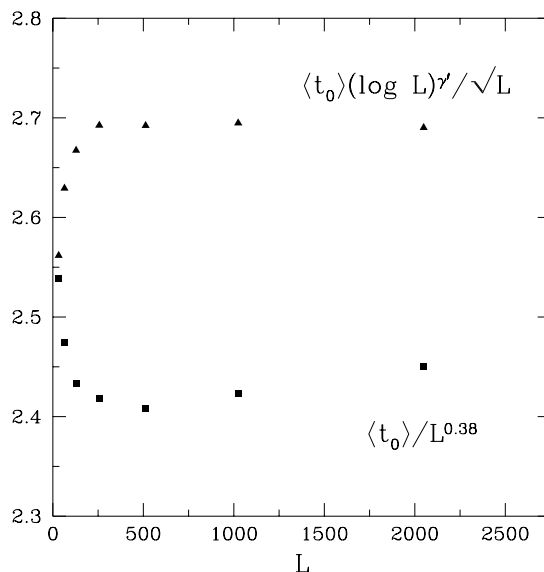


FIG. 11. Plot of $\langle t_0 \rangle / L^{0.38}$ (squares) and $\langle t_0 \rangle (\log L)^{\gamma'} / \sqrt{L}$, $\gamma' \simeq 0.74$ (triangles) as a function of L at the critical point in the 1d, biased case. The variation of $\langle t_0 \rangle$ as \sqrt{L} with multiplicative logarithmic correction seems to be a better fit than the fit to a pure power law. The plot of $\langle t_0 \rangle / L^{0.38}$ vs. L has been scaled by a constant factor. Set of parameters used: $\rho = 1, w = \rho L / (L - 1)$.

A good fit is obtained if one allows for logarithmic corrections in the power laws for $\langle M_0 \rangle$ and $\langle t_0 \rangle$ with $\beta = \gamma = 1/2$ (see Fig. 10 and Fig. 11). This indicates that both $\langle M_0 \rangle$ and $\langle t_0 \rangle$ vary as \sqrt{L} with multiplicative logarithmic corrections. Using Eq.(5) and the condition of criticality, one can easily show that $\eta + \beta - \gamma = 1$. Using $\beta = \gamma = 1/2$ as suggested by the discussion above, we obtain $\eta = 1$. The above quoted values for the exponents β and γ are consistent with the scaling relation $\beta + \gamma = 1$ which seems to be true in the NA and the PA phase as well. In the NA phase, we have seen in Section IV B that this scaling relation holds. In the PA phase, we found numerically that $\langle t_0 \rangle$ is independent of L in the thermodynamic limit implying that $\gamma = 0$; further since $\beta = 1$, it follows that the scaling relation $\beta + \gamma = 1$ holds in this phase also.

We have also numerically studied $P(t_1)$ which is the probability that the origin is occupied for t_1 consecutive time steps. At the critical point, this distribution shows two peaks – a broad peak occurs at the typical time scale $t_1 \sim L^\beta$ while there is a narrow peak at $t_1 = N_p/w$. We have not been able to reliably separate out these two contributions to $P(t_1)$ but since the scaling relation yields $\eta = 1$, one may expect that the second peak dominates the asymptotic value of η .

V. SINGLE-CHIPPER FREE PARTICLE MODEL

A. The Model

In this Section, we study the steady state of a model of noninteracting particles in which a localised infinite aggregate is formed solely due to disorder. In this model the particles diffuse freely in the bulk except at certain, quenched sites referred to as the chipper sites. It can be shown that this system exhibits a phase transition from the NA phase to the PA phase (as defined in Section II B) as the particle density is increased in all dimensions for all bias. In this Section, we will demonstrate this result in the presence of a single chipper. We will see that even a single defect is capable of inducing a phase transition in all dimensions, unlike in the aggregation model. We will discuss the solution with an extensive number of chipper sites in Section VI.

Our model is defined on a d -dimensional hypercubic lattice with periodic boundary conditions on which we consider the biased and unbiased diffusion of a conserved number of particles. At any site except the chipper, each particle attempts to hop out at rate 1. Since the particles do not interact, the hopping rate out of site k occupied by m particles is m . At the chipper site, assumed to be at the origin, the hopping rate is a constant w , independent of the number of particles. Thus, the rate $u_k(m)$ at which a particle leaves site k which has m particles is given by

$$u_k(m) = w \delta_{k,0} + m(1 - \delta_{k,0}) \quad , \quad m \neq 0 \quad . \quad (29)$$

In the fully asymmetric, $1d$ case, the model described above can be mapped onto a traffic model on a one lane road with no overtaking allowed. We represent each site in this model as a car and each particle as a vacant site. Then a system of M free particles on a lattice of size L maps onto a system of L particles with hard core interactions on a lattice of size $L + M$. In this new representation, the special car (corresponding to the chipper site) moves with a constant rate, irrespective of the headway in front of it and rest of the cars (sites other than the chipper) move with a rate proportional to the headway in front of it. Note that the *sitewise* disorder in the free particle model corresponds to *particlewise* disorder in the traffic model.

B. Phase Transition in arbitrary dimensions

The steady state of this system can be found exactly by noting that the hopping rates Eq.(29) in this model correspond to a special choice of rates in the Zero Range Process [18,14]. In this process, a particle at site k hops to its nearest neighbour independent of the state at the target site, so that the interaction has zero range. The steady state measure of this process can be found in any dimension with or without bias. A convenient way to find it is by using the condition of pairwise balance [24] which states that for any given configuration C , one can find a configuration C' in one-to-one correspondence with C'' such that

$$W(C' \rightarrow C) P(C') = W(C \rightarrow C'') P(C) \quad , \quad (30)$$

where $P(C)$ is the probability of a configuration C in a system with N sites and $W(C \rightarrow C')$ is the transition rate from C to C' . The above condition is satisfied by

$$P(C) = \frac{1}{\mathcal{N}} \prod_{k=1}^N f_k(m) \quad , \quad (31)$$

where

$$\begin{aligned} f_k(m) &= \prod_{i=1}^m \frac{1}{u_k(i)} \quad \text{for } m > 0 \\ &= 1 \quad \text{for } m = 0 \quad , \end{aligned} \quad (32)$$

and $u_k(m)$ is the rate at which a particle hops out of a site k having m particles and \mathcal{N} is the normalisation constant. $f_k(m)$ is defined upto a multiplicative factor v^m where v can be interpreted as the fugacity.

For our model, using the above solution for the particle distribution $f_k(m)$ and Eq.(29), we find that the normalised probability distribution $P_k(m)$ that the site k in the bulk has m particles has the Poisson form,

$$P_k(m) = P(m) = \frac{e^{-v} v^m}{m!} \quad , \quad k \neq 0 \quad . \quad (33)$$

The fugacity v will be determined using the conservation law. At the chipper site, one can obtain solution for $P_0(m)$ when $v < w$,

$$P_0^{NA}(m) = \left(1 - \frac{v}{w}\right) \left(\frac{v}{w}\right)^m \quad , \quad \frac{v}{w} < 1 \quad , \quad (34)$$

where NA in the superscript stands for the Non-Aggregate phase which we have added in the anticipation of a phase transition.

Using equations Eq.(33) and Eq.(34), one can easily see that the average particle number at site $k \neq 0$ is $\langle m_k \rangle = v = ws_0$ which further leads to constraint equation Eq.(5). Since this constraint equation is identical to that in the aggregation model, then as discussed in Section II B, the steady state of this model also has three possible phases (see Fig. 2). But, as we will see, this system never exists in the UA phase and there is a phase transition from the NA phase to the PA phase as ρ is increased, keeping w fixed, in all dimensions, irrespective of bias.

Solving for the average number of particles at the origin $\langle M_0 \rangle$ using Eq.(34) and substituting in Eq.(5), we obtain

$$\frac{s_0}{1-s_0} = \rho L^d - ws_0(L^d - 1) \quad , \quad 0 \leq s_0 < 1 \quad . \quad (35)$$

To leading order in L , one obtains two solutions, namely, $s_0 = \rho/w$ and $s_0 = 1$. Since the above analysis holds only when s_0 is strictly less than 1, the only valid solution is $s_0 = \rho/w$ for $\rho < w$. For $\rho \geq w$, s_0 is pinned to its maximum value 1. Thus there is a phase transition from the NA phase to the PA phase at $\rho_c = w$, as ρ is increased, keeping w fixed.

One can solve for $P_0(m)$ in the PA phase and at the critical point using the conservation law Eq.(5) and the fact that Eq.(33) is valid for all s_0 in the range $[0,1]$. Since the total number of particles is conserved, $P_0(m) = \sum_C P(C) \delta(\sum_{k \neq 0} m_k = M - m)$. The quantity on the RHS can be calculated straightforwardly. The result is

$$P_0^{PA}(m) = \sqrt{\frac{1}{\pi \langle m^2 \rangle (L^d - 1)}} \exp\left(-\frac{(M - m - \langle m \rangle (L^d - 1))^2}{(L^d - 1) \langle m^2 \rangle}\right) \quad , \quad (36)$$

where $\langle m \rangle = v$ and $\langle m^2 \rangle = v(1+v)$ from Eq.(33). One can see from the above equation that $\langle M_0 \rangle = M - w(L^d - 1) \sim L^d$ and $P_0^{PA}(0) = 1 - s_0 \sim e^{-L^d}$ in the PA phase. Further, at the critical point, we have $\rho L^d = w(L^d - 1)$ using which in Eq.(36), one obtains $P_0(m)$ at the critical point,

$$P_0^{cp}(m) = \sqrt{\frac{4}{\pi \langle m^2 \rangle (L^d - 1)}} \exp\left(-\frac{m^2}{(L^d - 1) \langle m^2 \rangle}\right) \quad , \quad (37)$$

which gives a power law decay in L for $P_0^{cp}(0)$.

The phase transition is brought about in this model in the following way. In the NA phase which is a low density phase, the typical number of particles at all sites including the chipper is of $O(1)$. As the density is increased, there is a phase transition to the PA phase at $\rho_c = w$. In this high density phase, each site in the bulk still supports only $O(1)$ number of particles in accordance with Eq.(33) so that the extra particles condense on the chipper giving rise to $\langle M_0 \rangle \sim L^d$. The mechanism of phase transition in this model is similar to that in Bose-Einstein condensation as was pointed out in [10] in a similar $1d$ model which shows a phase transition with $u_k(m) = w \delta_{k,0} + (1 - \delta_{k,0})$.

VI. EXTENSIVE DISORDER

In this Section, we describe a possible scenario in the more interesting and physically relevant situation when there is an extensive number of chipper sites. These are assumed to be placed randomly, with quenched random chipping rates w_k at site k distributed according to a distribution $\text{Prob}(w_k)$. We are interested primarily in the aggregation model but as argued below, on large space and time scales the behaviour of this model with extensive disorder resembles that of the corresponding free particle model (a generalization of the model in Section V with an extensive number of chippers) which is exactly solvable.

Let us consider the diffusion-aggregation process with no bias and take the initial condition to have a random distribution of masses. Then the finite concentration c of chipper sites brings in new length and time scales into the problem, namely the mean spacing $l_c \sim c^{1/d}$ between the chippers and the associated diffusion time $t_c = l_c^2$. Evidently, l_c and t_c define respectively the relevant length and time scales over which the diffusing mass clusters sense the presence of an extensive number of defects.

Let us consider a finite but low concentration of chipper sites so that $1 \ll l_c \ll L$. On time scales $t \ll t_c$, we would expect the system to behave roughly as independent, finite systems of size l_c with typically a single chipper each. The typical state on these short time scales thus resembles the UA-like steady state discussed in Section III. The typical mass of clusters, both mobile and localised is limited by the time and grows proportional to $t^{d/2}$ as long as $t \ll t_c$.

As the time crosses t_c , the finite spacing between the chippers becomes relevant. The primary effect is to limit the size of the aggregates formed in the non-chipper region by the diffusion-aggregation process to $\sim l_c^d$, since on a time scale $\gtrsim t_c$ the mass cluster is likely to encounter a chipper and get trapped. For $t \gg t_c$, the coarse grained view of the system is that of mass exchanged between close-by random rate chippers with each exchange taking a time $\sim t_c$. To the extent that only finite aggregates (with mass $\sim l_c^d \ll L^d$) are formed in the transit between chippers, it is plausible that on large length and time scales, we may ignore interaction effects (i.e. coalescence) and think of the system as effectively free-particle like in the non-chipper region.

The free particle model with extensive disorder is solvable along the same lines as the single-chipper problem described in Section V. It defines a Zero Range Process with the hopping rates,

$$\begin{aligned} u_k(m) &= w_k \quad , \quad \text{if } k \text{ is a chipper site} \\ &= m \quad , \quad \text{if } k \text{ is not a chipper site} \end{aligned} \quad (38)$$

Let x denote the fraction of chipper sites. We recover the single-chipper model as $x \rightarrow 0$, while $x \rightarrow 1$ corresponds to every site being a chipper site, and is the model considered in [9,10]. For all x , in the low-density phase, the mass distribution on the non-chipper sites follows the probability distribution of Eq.(33), while at chipper sites, Eq.(34) is valid with w replaced by w_k . Let s_k be the occupation probability of site k , and s_0 refer to the occupation probability of the site with the lowest chipping rate, $w_0 = \text{Min}\{w_k\}$. Then in the steady state, the spatial uniformity of the current leads to (i) $w_k s_k = w_0 s_0$ if k is a chipper site, and (ii) $\langle m_k \rangle = w_0 s_0$ if k is not a chipper site. Using these relations, one can write the mass conservation equation analogous to Eq.(35) as

$$\frac{1}{L^d} \frac{s_0}{1-s_0} + x \int dw \frac{\text{Prob}(w)s_0}{w/w_0 - s_0} + (1-x)s_0 w_0 = \rho \quad . \quad (39)$$

where we have separated out the first term corresponding to the slowest chipper.

One can analyse Eq.(39) for various x as follows: (a) In the limit of a single chipper (reached as x approaches 0), we know from Section V that as the density is increased, there is a phase transition from the NA phase to the PA phase with an infinite aggregate at the chipper site. (b) In the limit $x \rightarrow 1$, the model reduces to that considered in [9,10], where it is shown that for $\text{Prob}(w_k) \sim (w_k - w_0)^\nu$ as $w_k \rightarrow w_0$, the system stays in the NA phase for all ρ if $\nu \leq 0$. On the other hand, if $\nu > 0$, then there is a transition to the PA phase with an infinite aggregate at the site with chipping rate w_0 when the density crosses the critical density given by

$$\rho_c(x=1) = \int dw \frac{\text{Prob}(w)}{w/w_0 - 1} \quad . \quad (40)$$

(c) For $0 < x < 1$, there is a transition from the NA to the PA phase if $\text{Prob}(w)$ is chosen as in (b) above. The critical density can be determined by taking $s_0 \rightarrow 1$ and $L^d(1-s_0) \rightarrow \infty$ in Eq.(39), with the result

$$\rho_c(x) = x\rho_c(x=1) + (1-x)w_0 \quad . \quad (41)$$

Thus the critical density interpolates linearly between its values in the limits $x=0$ and $x=1$.

In view of the correspondence discussed at the beginning of this Section, we would expect the aggregation model with a similar distribution of chipper sites to show a phase transition from the NA to the PA phase. In the former phase, there are both localized and mobile aggregates with typical mass $\sim l_c^d$. In the PA phase, the distribution of masses is similar to that in the NA phase at all sites except the slowest chipper with $w_k = w_0$; at this slowest site, there is an aggregate with mass of order volume.

VII. SUMMARY

In this paper, we introduced a minimal model to study the effect of quenched, sitewise disorder in an aggregation-fragmentation system. Our model had some simplifications: the fragmentation was allowed to occur only at the trapping sites, and mass-independent kernels for aggregation and fragmentation were considered. Despite these simplifications, it retains the important physical effects of diffusion, aggregation, fragmentation and trapping.

We studied the case of a single-chipper aggregation model in detail. In all cases except the $1d$, biased case, the system exists in the UA phase in which an infinite aggregate localised at the chipper site can coexist with mobile infinite aggregates in the bulk. The simultaneous existence of more than one infinite aggregate is a new feature absent in previous studies of translationally invariant systems. In the $1d$, biased case, there is a phase transition from a phase in which a localised aggregate is formed at the chipper site (PA phase) to the one in which no aggregate is formed anywhere in the system (NA phase) as the density is decreased.

We also studied a variant of the above aggregation model in which particles chip off at a single site but diffuse freely in the bulk. This model can be solved exactly and shows a phase transition from the PA phase to the NA phase as density is increased in all dimensions for all bias.

Finally we discussed a likely scenario for the aggregation model in the presence of extensive disorder and argued that interaction effects arising due to coalescence can be ignored on large enough time scales. It would be interesting to check this expectation by a more detailed study of the system with extensive disorder.

Acknowledgements: We thank D. Dhar and Rajesh R. for useful discussions and comments on an earlier version of the manuscript.

-
- [1] R. M. Ziff, *J. Stat. Phys.* **23**, 241 (1980).
 - [2] *Smoke, Dust and Haze: Fundamentals of aerosols dynamics (2nd ed.)*, S. K. Friedlander. (Oxford University Press, 2000)
 - [3] See the articles by S. Redner, D. ben-Avraham and M. Takayasu and H. Takayasu in *Nonequilibrium Statistical Mechanics in One Dimension*, V. Privman, ed. (Cambridge University Press, Cambridge, 1997).
 - [4] H. Takayasu and Y-h. Taguchi, *Phys. Rev. Lett.* **70**, 782 (1993).
 - [5] P. L. Krapivsky and S. Redner, *Phys. Rev. E* **54**, 3553 (1996), cond-mat/9509129.
 - [6] S.N. Majumdar, S. Krishnamurthy and M. Barma, *Phys. Rev. Lett.* **81**, 3691 (1998).
 - [7] S.N. Majumdar, S. Krishnamurthy and M. Barma, *J. Stat. Phys.* **99**, 1 (2000).
 - [8] R. Rajesh and S. N. Majumdar, cond-mat/0009110.
 - [9] J. Krug and P. Ferrari, *J. Phys. A* **29**, L465 (1996).
 - [10] M. R. Evans, *Europhys. Lett.* **36**, 13 (1996); M. R. Evans, *J. Phys. A* **30**, 5669 (1997).
 - [11] G. Tripathy and M. Barma, *Phys. Rev. Lett.* **78**, 3039 (1997); *Phys. Rev. E* **58**, 1911 (1998).
 - [12] B. Derrida, S. A. Janowsky, J. L. Lebowitz and E. R. Speer, *Europhys. Lett.* **22**, 651; P. F. Arndt, T. Heinzel and V. Rittenberg, *J. Phys. A: Math. Gen.* **31**, 833 (1998).
 - [13] For a recent review on disordered exclusion models, see J. Krug, cond-mat/9912411.
 - [14] M. R. Evans, *Brazilian Journal of Physics*, **30**, 42 (2000), cond-mat/0007293, and references therein.
 - [15] S. A. Janowsky and J. L. Lebowitz, *Phys. Rev. A* **45**, 618 (1992).
 - [16] G. Schütz, *J. Stat. Phys.* **71**, 471 (1993).
 - [17] K. Mallick, *J. Phys. A: Math. Gen.* **29**, 5375 (1996).
 - [18] F. Spitzer, *Adv. in Math.* **5**, 246 (1970).
 - [19] For the $1d$, biased case, the MFT result for mean-squared mass is $\langle m_k^2 \rangle = Lf(k/L)$ where $f(x) \sim x$. Thus MFT is sensitive to bias in this case unlike the translationally invariant cases (see [7] for example) in which the mean field equations are independent of the bias.
 - [20] B. Derrida, V. Hakim and V. Pasquier, *Phys. Rev. Lett.* **75**, 751 (1995).
 - [21] Z. Cheng, S. Redner and F. Leyvraz, *Phys. Rev. Lett.* **62**, 2321 (1989).

- [22] D. ben-Avraham, M. A. Burschka and C. R. Doering, *J. Stat. Phys.* **60**, 695 (1990).
- [23] R. Rajesh and S. N. Majumdar, *cond-mat/9910206*.
- [24] G. Schütz, R. Ramaswamy and M. Barma, *J. Phys. A* **29**, 837 (1996).